ADVANCED 3D FINITE ELEMENT SIMULATION OF THERMOPLASTIC COMPOSITE INDUCTION WELDING

Miro Duhovic[1], Pierre L'Eplattenier[2], Iñaki Caldichoury[2] and Joachim Hausmann[1]

[1]Institut für Verbundwerkstoffe GmbH, Erwin-Schrödinger-Str., Gebäude 58, 67663 Kaiserslautern, Germany
Email: miro.duhovic@ivw.uni-kl.de, joachim.hausmann@ivw.uni-kl.de, web page: http://www.ivw.uni-kl.de

[2] Livermore Software Technology Corporation, 7374 Las Positas Road, Livermore, CA 94661, USA
Email: pierre@lstc.com, inaki@lstc.com, web page: http://www.lstc.com

Keywords: CFRTP, Induction welding, Finite element simulation

ABSTRACT

The joining of carbon fiber reinforced thermoplastic (CFRTP) composites via electromagnetic (EM) induction welding is a complex multi-physics problem making the process very difficult to study by experiments alone. With the correct combination of experiments and simulations a more complete understanding of the process can be achieved together with an insight into which parameters need to be adjusted in order to optimize the process. The key elements of an induction welding simulation can be demonstrated using single plate heating models. Comparisons can also be made with double plate heating simulations whereby electrical and thermal contact resistance can also be taken into account. In the present work, finite element analysis (FEA) methods have been used to simulate single and double plate static induction heating of carbon fiber based thermoplastic composite laminates with a 2 mm thickness. The static plate heating tests are validated using the finite element simulation software LS-DYNA® by comparing point temperature measurements through the thickness of the specimens. Following on from the static experiments, a simulation test-bed has been created in order to study the continuous induction welding of two joining partners allowing the generation of 3D surface plots of temperatures through the thickness of the joint and most importantly at the joining interface. This information can then be used to assess the degree of bonding between the joining partners and overall quality of the weld.

1 INTRODUCTION

In 2015, the automotive industry has still only just begun to integrate fiber reinforce plastics (FRPs) into vehicles. It can be foreseen that in the future more and more individual parts will be designed and manufactured from FRPs. These parts will be expected to function synergistically with other materials such as advanced metals as has already occurred in the aerospace industry. With these developments in mind, mass production ready manufacturing techniques for FRPs will become of the utmost importance. One type of FRP showing the greatest potential for mass production are the continuous fiber reinforced semi-finished sheets or so called "organosheet" materials. These thermoplastic composites show processing potential similar to that of sheet metals. Shaping can be achieved via thermoforming and joining by fusion bonding (welding) using equipment close to that currently used for metals and making them a very attractive material addition for mass production.

Induction welding is one efficient means of joining such materials but involves many interacting parameters and is difficult to study let alone optimize by experiments alone. Many of the well-known general purpose finite element software codes are today becoming capable of multi-physics simulations and can help. The aim of this process modeling case is to be able to predict the optimal processing parameters of a continuous induction welding process. The input variables are the electromagnetic and thermal properties of both the material undergoing the heating and the induction coil which is part of the welding system. In addition, the electromagnetic and thermodynamic

constraints of the surrounding environment (which is usually air) is also accounted for. The generator input parameters (e.g. frequency, coil current, coupling distance) are also required. Some of these parameters can be taken from the literature or databases, while others such as the generator input parameters can be measured directly from the induction heating equipment itself. One of the most critical set of input parameters is that of the laminate material itself. Here the parameters need to be measured using mechanical, thermal and electromagnetic material characterization experiments.

2 INDUCTION WELDING BASICS

The basic principle of induction heating/welding can be described as illustrated in Figure 1. Here the induction coil which is connected to a high frequency alternating current source (usually in the kHz – MHz range) creates a magnetic field within its near surroundings. The alternating magnetic field induces eddy currents in the workpiece (in this case the carbon fiber reinforced plastic (CFRP)) when placed in close proximity to the coil. Heat energy is then generated via the Joule effect as a result of the induced eddy currents flowing through the electrically conductive material [1, 2]. Composites containing carbon fibers in certain configurations (in particular woven structures) also produce a Joule heating effect and can be utilized to create the heat energy necessary for welding. The subsequent adhesion is then supported by applying pressure and allowing enough time for fusion bonding to take place.

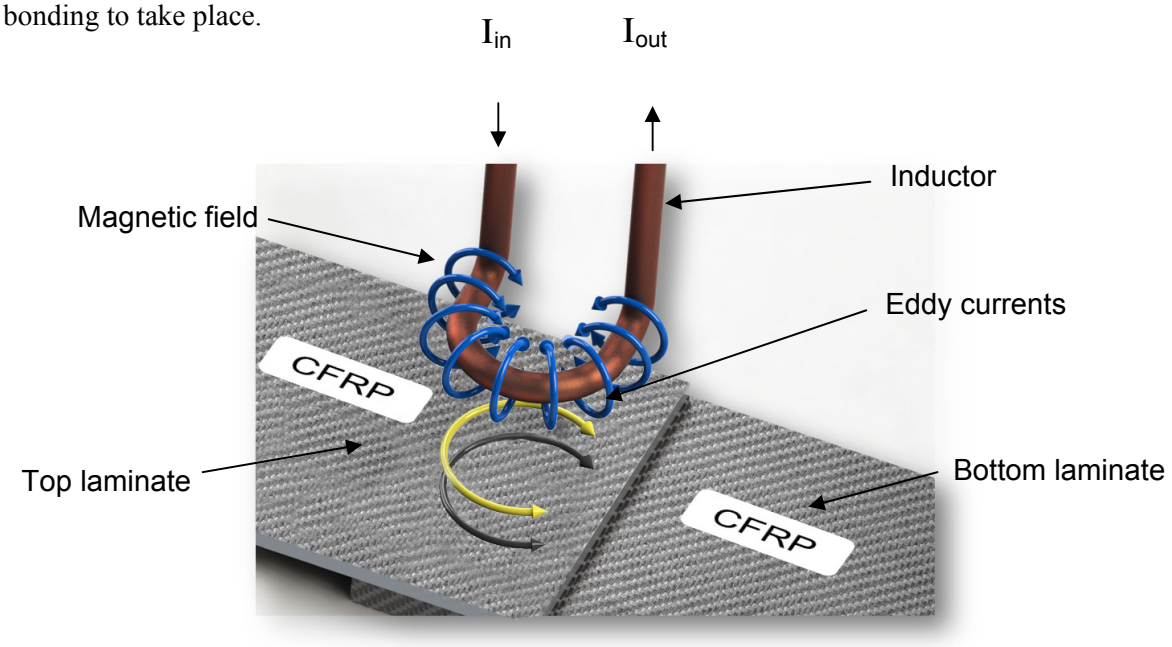

Figure 1: Induction heating principle for CFRP material joints (courtesy of Mrs. Mirja Didi, IVW GmbH).

During a finite element simulation of the induction welding process, it is precisely this Joule heating phenomena which is of primary interest to be simulated. Moreover, knowledge about the heating, cooling, and pressure time history at the joint interface is exactly what is required in order to be able to predict the final joint strength. How these variables can be used to estimate the joint strength is a detailed topic in itself involving the theories of 'intimate contact' and 'autohesion' (or healing) as has been proposed by Loos et al. [3], Lee et al. [4] and later Yang and Pitchumani [5-7] and will not be covered here. It is safe to say, that only after the correct prediction of all the manufacturing phenomena which occur during induction welding is achieved, does it make sense to proceed onwards in this direction.

3 MATERIAL PROPERTIES

The most important inputs to any simulation are the material properties. To simulate induction welding a wide variety of material properties are required in order to capture all of the physics

involved. Table 1 shows some of the typical mechanical, thermal and electromagnetic properties used, many of which (for example, the material stiffness, heat capacity, thermal conductivity, electrical conductivity and magnetic permeability) can be defined with temperature dependency. In some cases the temperature dependence is not significant and can be ignored. This is the case, for example, with the thermal conductivity in CFRPs since its overall magnitude and resulting influence on the induction heating effect is very low. For other multi-physics parameters such as the material stiffness, heat capacity and the electrical conductivity, defining temperature dependent properties are crucial towards achieving the correct results.

Type of Physics	Material Property		Air	Coil (Copper)	Composite Plate (*CF-PPS)
Mech.	Stiffness, E (Pa)	E_1, ν_1	-	1.1×10^{11}, 0.34	6.0×10^{10}, 0.35 E, v vs. T curve
		E_2, ν_2	-		6.0×10^{10}, 0.35 E, v vs. T curve
		E_3, ν_3	-		4.0×10^{10}, 0.35 E, v vs. T curve
	Density, ρ (kg/m^3)		1.293	8960	1790
Therm.	Heat Capacity at (const. pressure), Cp (J/(kg*K)		1010	385	[1]1803 Cp vs. T curve
	Thermal Conductivity, k (W/m*K)	k_1	0.026	390	[2]2.50
		k_2	-	-	[2]2.50
		k_3	-	-	[2]0.32
EM	Electrical Conductivity, σ (S/m)	σ_1	1	5.998×10^7	[3]1.389×10^4 σ vs. T curve
		σ_2			[3]1.389×10^4 σ vs. T curve
		σ_3			[3]1.000×10^1 σ vs. T curve
	Relative Permittivity, ε_r		1	1	[4]3.7
	Relative Permeability, μ_r		1	1	1 B vs. H curve μ_r vs. T curve
	Surface Emissivity (Radiation)		-	0.5	0.95
	Skin Depth (mm) (automatically calculated)		-	~ 0.1	~ 3.5

[1,2,3,4] *Values taken from the measurements and data collected from the work of references [8, 9, 10].*
**Carbon fiber reinforced polyphenylene sulfide*

Table 1: Summary of typical material property parameters used in the developed LS-DYNA® induction heating finite element models.

While it is obvious that the CFRP's thermal properties are and should be considered orthotropic, the question of whether or not orthotropic electrical conductivity should be considered also arises. In the most complex case, a temperature dependent orthotropic material property input may be required. An attempt to answer this question is given in Section 4.2. In addition to the material properties, boundary conditions such as the thermal contact heat transfer coefficient, contact resistivity, and temperature dependent radiation and convection coefficients on the exposed surfaces of the plates are important and all play a significant role in predicting the correct temperature distribution.

4 STATIC PLATE HEATING CHARACTERIZATION

4.1 Single and double plate heating models

The key elements of an induction welding simulation can be demonstrated using static plate heating models. Comparisons can be made with both single and double plate heating simulations whereby in the latter the influence of a contact resistance can also be considered. Figures 2 a) and b) show example models and point temperature heating results of single and double (100 x 100 x 2 mm) CF-PPS static plate induction heating simulations compared to their corresponding experiments. Note that in the images the models have been cut in half in order to better visualize the through thickness temperatures.

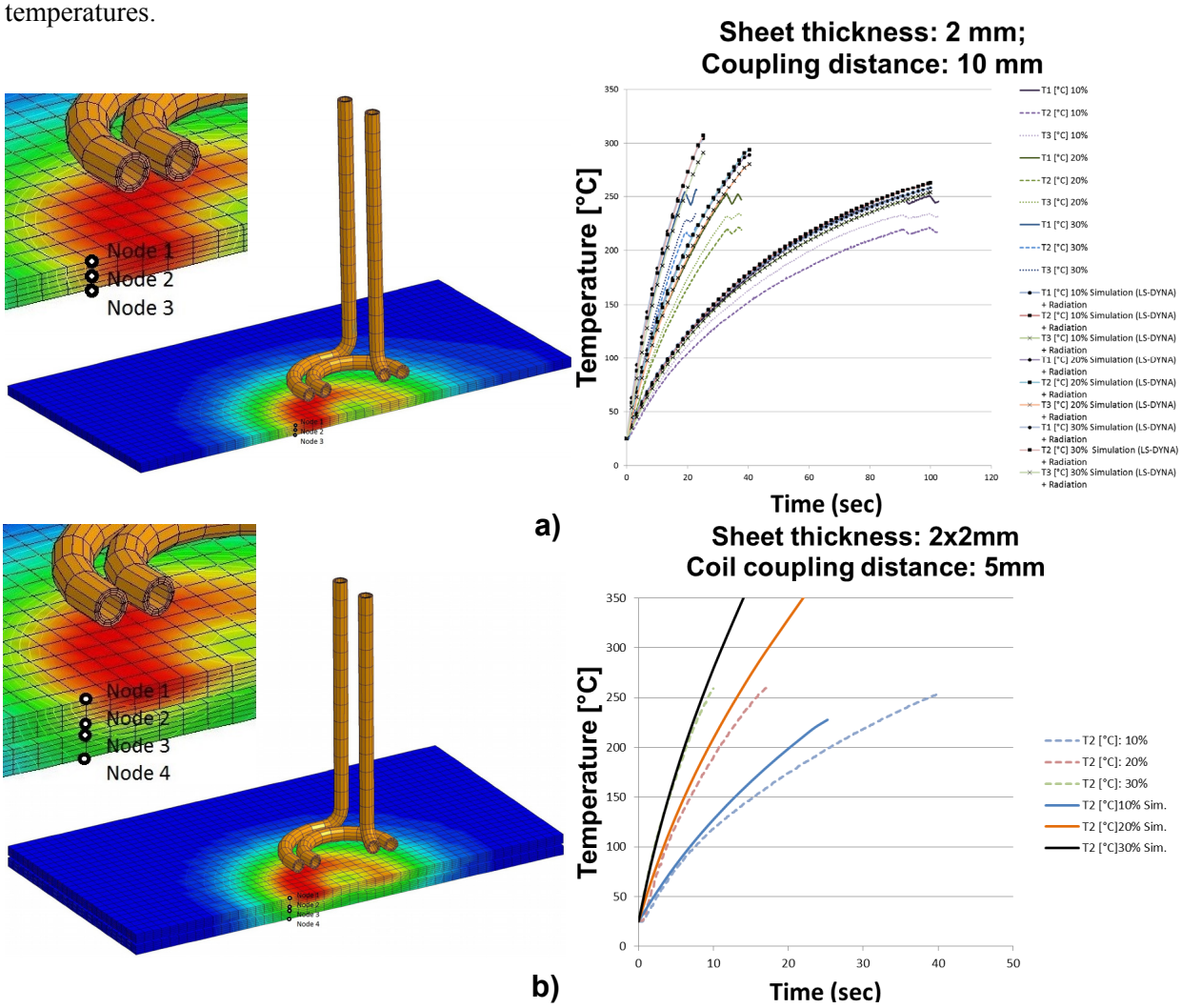

Figure 2: FEM/BEM simulation model set-up for a) single and b) double plate through the thickness temperature investigations and their corresponding point temperature comparisons between experiments and LS-DYNA simulation results at 10% (163 A), 20% (231 A) and 30% (283 A) power and a coil frequency of 540kHz.

The necessary geometry for both the coil and CFRP plate are both meshed to a suitable resolution to allow for the correct electromagnetic and thermal behavior of the system to be calculated. In the present models both the coil and plate geometries are meshed using solid hexahedral elements. The electromagnetic calculation is performed using the boundary element method (BEM) which solves Maxwell's equations in the eddy current induction diffusion approximation. The elements required for the BEM calculations are automatically generated on the surfaces of the solid finite element mesh which itself considers the thermal and mechanical effects in the usual way. Both types of elements are strongly coupled meaning that there is transfer of information (e.g. temperature) between the different

physics solvers operating on each type of elements.

Note that the node locations shown in Figure 2 correspond to the location of thermocouples ($T_{1,2,3}$ on the graph legend) used in the physical experiments. The heating of two plates is of more interest than one, but adds further complications as it involves an extra load contributor (i.e. an extra plate) in the electromagnetic circuit. The eddy currents developed in the top plate are now also affected by the presence of the bottom plate as well as the coil. In addition, the influence of a contact resistance may also be considered. In the double plate simulation case, nodes 2 and 3 have been averaged to estimate the experimental temperature T_2 at the joining interface.

4.2 Influence of non-linear electrical conductivity and orthotropic material input

In general, using a constant value of electrical conductivity over-predicts the heating effect over a wider temperature range as can be seen in Figure 2. By defining a non-linear electrical conductivity dependent on temperature, both the temperature spread through the thickness and the predictions over a large temperature range can be improved. This improvement however, comes at the expense of computing time as the electromagnetic fields must be recalculated enough times to capture the non-linearity.

Simulations performed to assess the significance of orthotropic electrical conductivity tend to suggest no difference in the heating behavior when the material is considered electrically orthotropic as opposed to isotropic. In an isotropic case, the material is assumed to have an electrical conductivity equivalent in all directions to that measured in the in-plane directions. It can only be presumed that the large order of magnitude difference (~1000) between the in-plane and through the thickness electrical conductivity, combined with the large skin depth (almost the entire thickness of the laminate stack) results in an insensitivity to the through thickness value of electrical conductivity. This means that a simpler (isotropic) electromagnetic material model can in this case be applied.

5 UNDERSTANDING THE CONTINUOUS INDUCTION WELDING PROCESS

The typical setup for the continuous joining of two composite laminates is illustrated in Figure 3. The graph in the figure presents the typical temperature profile of a fixed point on the top surface of the laminate stack during the induction welding procedure.

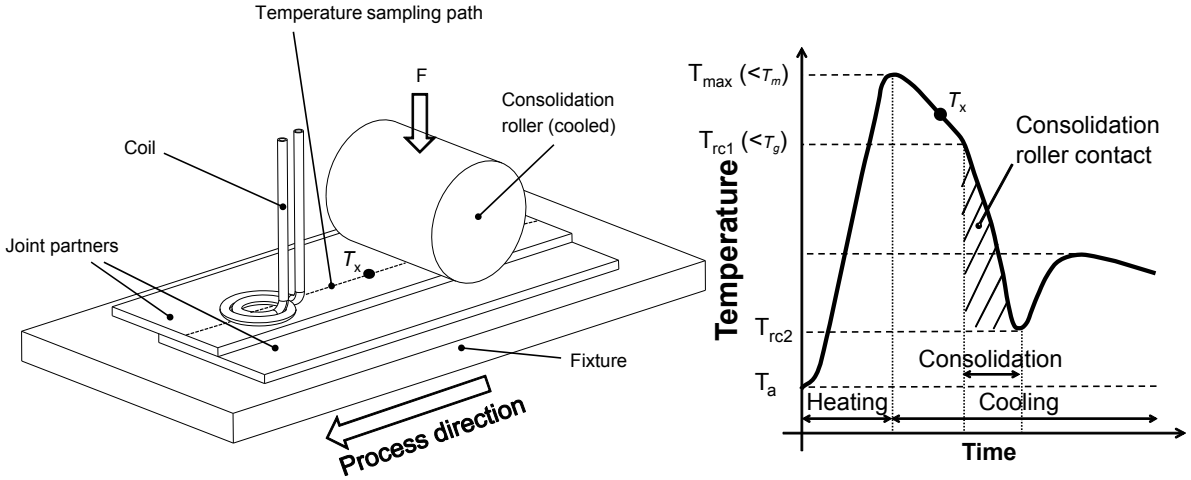

Figure 3: Setup for the continuous induction welding of two composite plates and simplified temperature versus time profile on the top surface of the laminate stack during continuous induction welding (based on data from Rudolf and Moser et al.[8, 9]).

The nature of the graph can be described as follows: As the material passes below the coil, its temperature rises until it reaches T_{max}, signifying the end of the heating phase of the process. The temperature then drops slightly due to heat transferred to the jig and surroundings via free convection, radiation and conduction until the roller first contacts the measurement point at T_{rc1}. Here the consolidation phase begins and the temperature drops steeply as the roller applies pressure and cools the material to T_{rc2}. Heat inertia resulting from the intrinsic heating then causes a slight rise in the temperature well below melt temperature after which the material then slowly cools back to the starting temperature T_a. Note that for ease of explanation, a point on the top surface of the welding stack has been considered. A similar shaped curve, but with less influence from the consolidation roller also exists at the joining interface, whereby T_{max} now, must be less than the degradation temperature of the polymer, T_d (rather than the melt temperature of the polymer, T_m) and T_{rc1} should be equal to or slightly above T_m. T_{rc2} should aim to cool the polymer to below the heat distortion temperature T_{HDT}, where there is no further need for the consolidation roller to apply pressure to the welding stack. In this way, the material has the time it needs to create the bond. For slow welding speeds in the order of 1-3 mm/sec this is easy to achieve. For processing speeds of up to 100-300 mm/sec (which would be deemed acceptable for mass production scenarios) difficulties arise. One of the goals of the test-bed simulation is to therefore analyze the possibilities of such welding speeds and to assess if and how these could possibly be achieved.

6 INDUCTION WELDING SIMULATION TEST-BED

All of the necessary features and physics of the continuous induction welding process have been captured in the developed simulation test-bed as shown in Figure 4. The simulation test-bed sets the stage for more complex finite element investigations using moving coil cases where the steady state induction heating temperature patterns become different to that of the static case and are far more difficult to predict and measure. Using this process simulation tool, the effects of the consolidation roller as well as an impinging air jet on the temperature developed on the top surface of the laminate stack, and more importantly the joint interface, can be investigated in full detail. Simulations can be carried out to gain a better understanding of the process and how to best go about optimizing it.

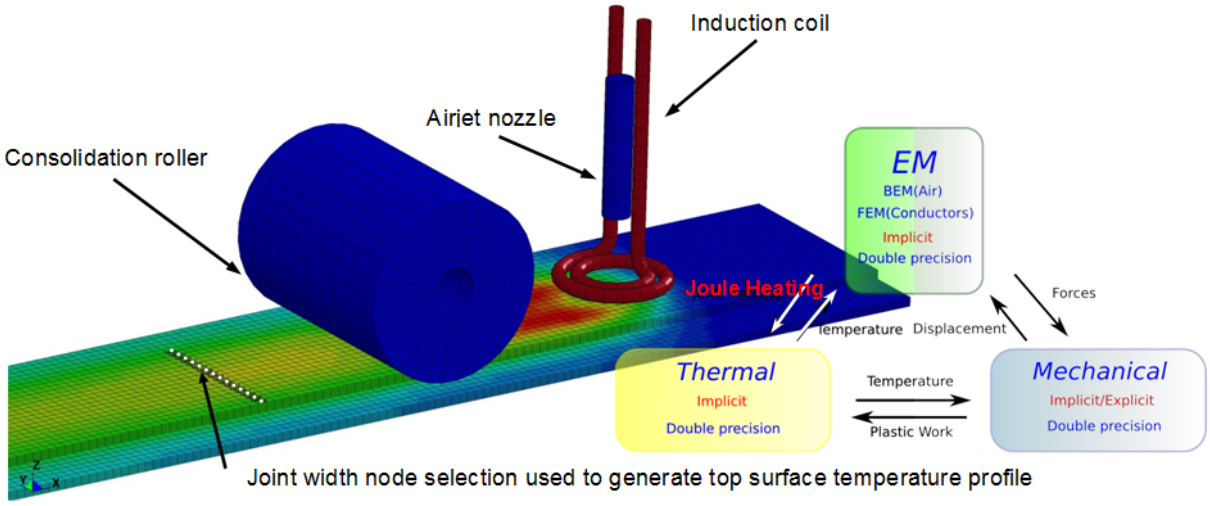

Figure 4: Simulation test-bed setup for the continuous induction welding of two material partners and their corresponding physics interactions developed at the Institut für Verbundwerkstoffe GmbH together with LSTC.

All of the necessary physics has been defined, including the joule heating resulting from the induction coil interacting with both the CFRP plates. A vertical consolidation roller contact force has been applied and together with a friction coefficient and a horizontal velocity boundary condition (which defines the processing speed) to enable the correct rolling motion. Heat transfer via convection

and radiation to the surrounding air as well as conduction to the consolidation roller is also considered. Finally, the heat transfer and pressure resulting from an air-jet is also simulated via a moving heat flux and moving pressure boundary conditions respectively. Further details about the model can be found in the previous works of Duhovic et al. [10, 11].

6.1 Influence of top surface cooling

In Figures 5 a) and b), the simulation test-bed is used to investigate the influence of top surface cooling on the temperature development of the top surface laminate during induction welding of CFRP (CF-PPS) organosheet for fixed power and frequency settings of 240 A and 400kHz respectively. It can be seen that the effect of the top surface cooling reduces the maximum temperature developed in the top plate by almost 200°C thereby avoiding any thermal damage on the plate surface closest to the induction coil.

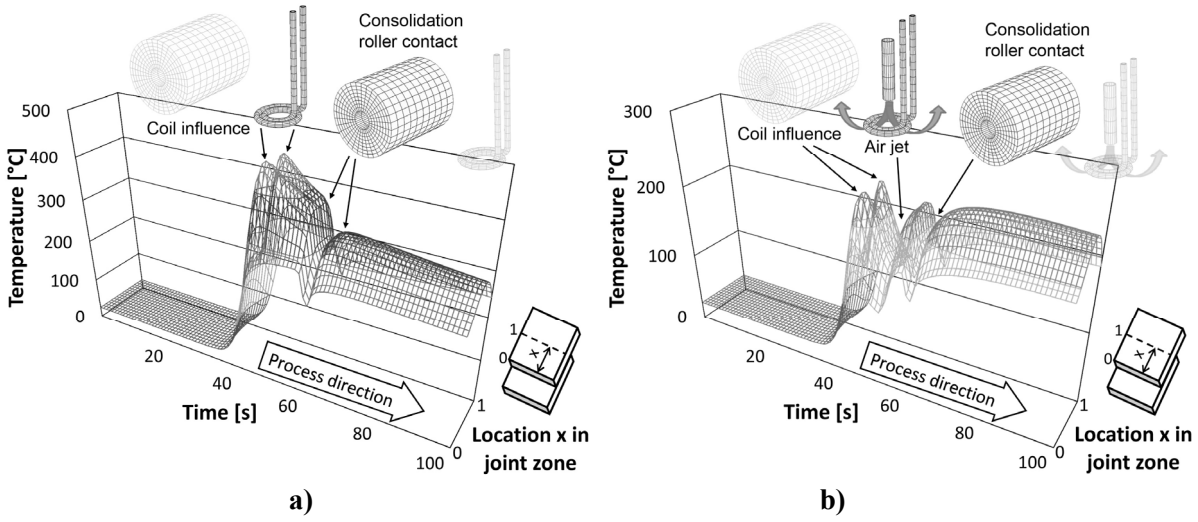

Figure 5: Top surface temperature plots for the top laminate using nodes selected across the entire width of the weld as shown in Figure 4, welding speed 3 mm/sec, fixed coil coupling distance 2 mm and coil to roller offset distance 60 mm; a) without and b) with air-jet cooling (304 liters/min).

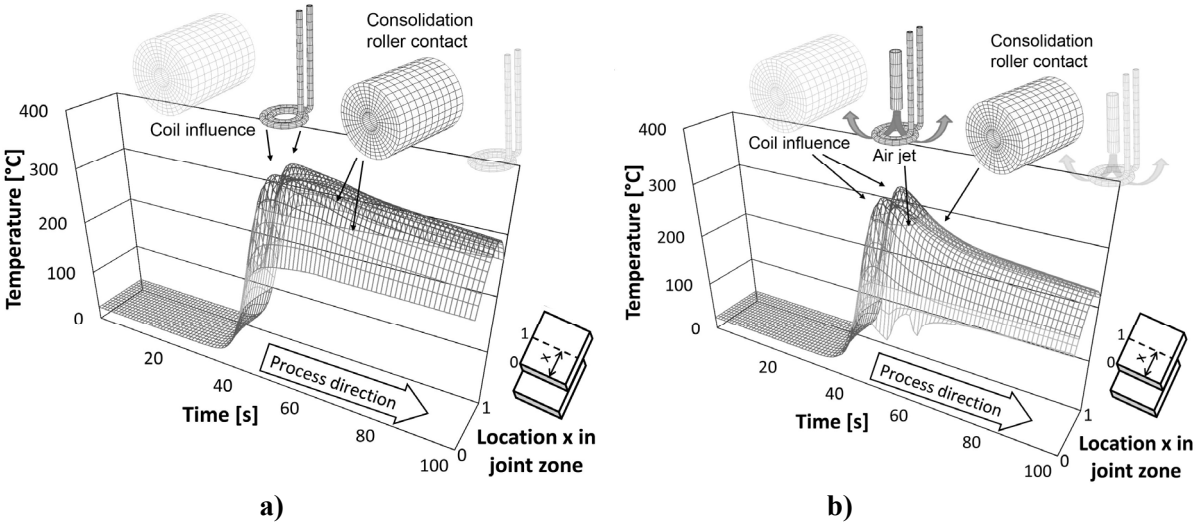

Figure 6: Bond-line surface temperature plot using nodes selected across the entire width of the weld as shown in Figure 4, welding speed 3 mm/sec, fixed coil coupling distance 2 mm and coil to roller offset distance 60 mm; a) without and b) with air-jet cooling (304 liters/min).

An equally favorable effect of the surface cooling on the bond-line surface temperature can be seen in Figures 6 a) and b). The surface plots here show that a larger drop in temperature is achieved over a shorter period of time as a result of the surface cooling, suggesting that better consolidation of the laminates should take place. In an ideal joining case, the goal would be that the temperatures across the width of the surface plot must all fall within the processing temperature window of the thermoplastic polymer material used, if complete adhesion of the overlapping area is desired. It can now be seen that this characteristic is strongly dependent on the nature of the heating pattern generated by the coil, or in other words, the coil geometry. To achieve faster welding speeds the heating non-uniformity of the coil across the width of the joint must therefore be kept to a minimum.

6.2 Influence of faster welding speed

It is interesting to examine what happens when a welding speed of 300 mm/sec, for example is simulated, the speed at which the process would become interesting for mass production implementation. The coil current in this case needs to be increased by a factor of 10 so that temperatures close to melting can be achieved and an air jet cooling flow rate of 304 liters/min is once again used. It can be seen from Figures 7 a) and 7 b) that regardless of the top surface cooling, the temperature plots of the top surface and in the bond line surface both show no drop in temperature, which means that no bonding can occur. In other words, due to the poor thermal conductivity of the laminate, the heat input cannot escape fast enough at this welding speed to create the conditions required for bonding to take place within the given timeframe. It can also be seen that the air-jet cooling of the top surface is no longer effective in keeping the temperature the below melting point and that a very wide temperature distribution across the width of the weld now exists.

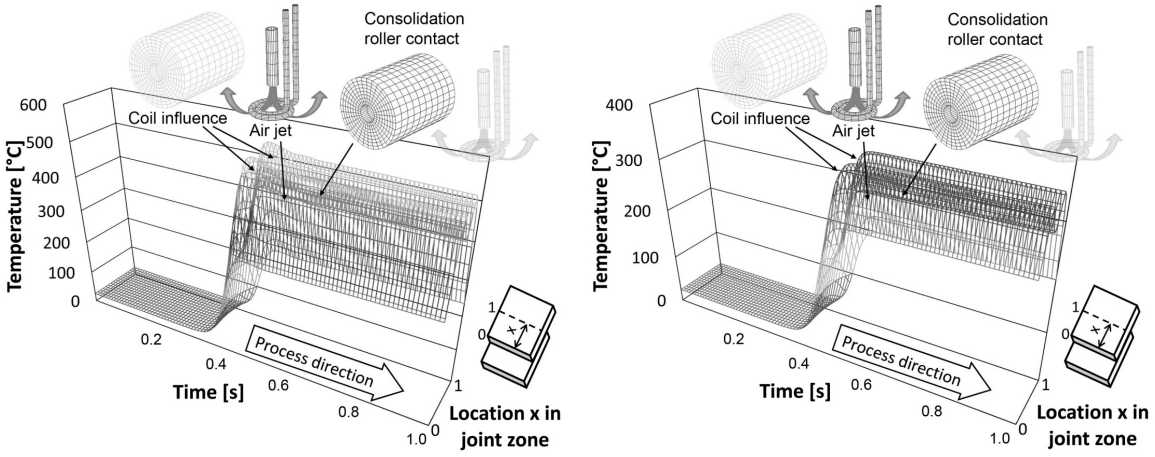

Figure 7: Top surface a) and bond-line b) surface temperature plots using nodes selected across the entire width of the weld as shown in Figure 4, welding speed 300 mm/sec, fixed coil coupling distance 2 mm and coil to roller offset distance 60 mm with air-jet cooling (304 liters/min).

6.3 Implementation of an induction welding control system

Choosing the correct coil current which yields the maximum allowable temperature in the welding stack is not a trivial task. Experimentally this is done by trial and error and the chosen value for the coil current is then by no means the optimum. Two types of control systems have been considered in the current simulation test-bed model, which correspond to that which would be possible to some degree also in reality. The first is a simple generator ON/OFF switch where the maximum temperature anywhere in the welding stack is monitored and the induction generator (the EM solver in the simulation) is switched off when a single node anywhere in the welding stack reaches a user defined upper limit. Likewise, the solver is switched back on when all of the nodes in the welding stack fall

below a user specified minimum value. A more sophisticated form of process regulation via proportional-integral-derivative (PID) control is also possible in the simulation. In this case, the maximum temperature in the welding stack is again monitored and provides continuous feedback values (maximum temperature values with respect to time) to the controller function. The available PID controller function in LS-DYNA® can then perform a type of closed-loop control as shown in Figure 8. Here the maximum temperature detected in the welding stack versus time and its corresponding coil current amplitude is presented for three different PID controller settings. This functionality can be used to automatically assign the correct steady state current amplitude in the process and also regulate it on the fly. In the future it is hoped that this can be used to find out automatically the correct current amplitude to apply in the case of welding at different speeds and for different and even dissimilar material combinations as well as compensate for disturbances when more complex geometries are welded.

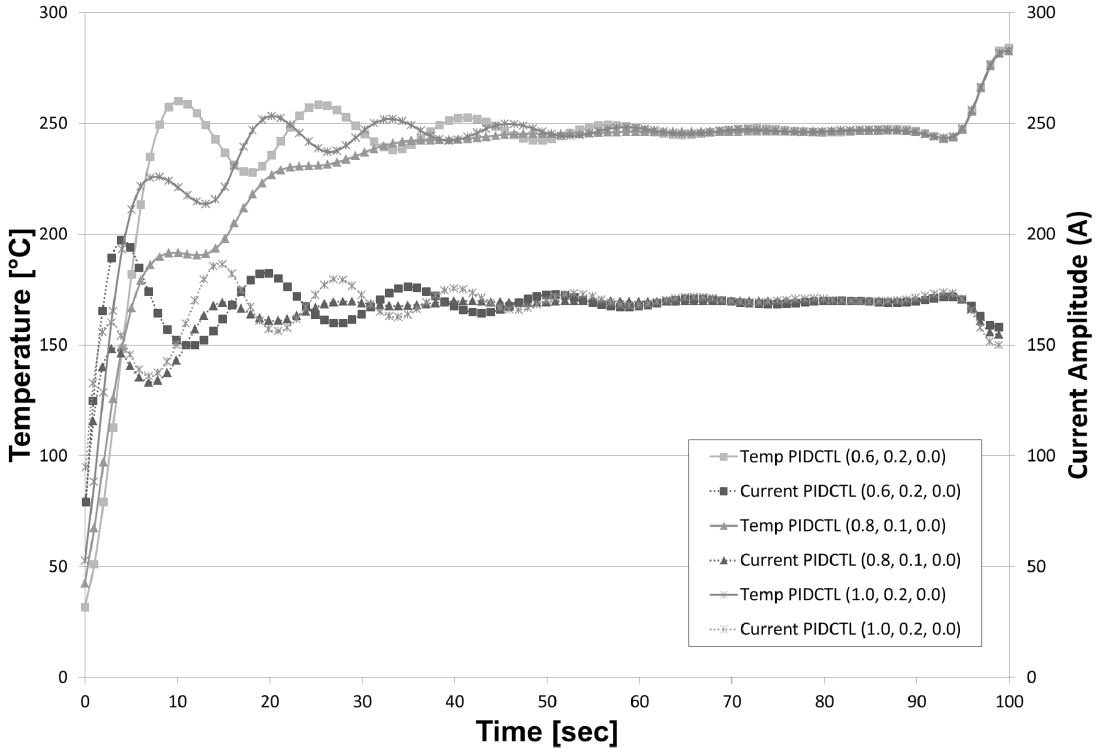

Figure 8: PID control enhanced test-bed simulation output allowing automatic adjustment of the coil current to achieve a user defined maximum temperature in welding stack of 250°C.

7 CONCLUSIONS

The present work has demonstrated some of the advanced 3D modelling techniques which can be used to help optimize the induction welding process of CFRP materials. A simulation test-bed investigating a two-dimensional induction welding procedure has been developed which considers all three types of physics (structural mechanics, heat transfer and electromagnetism) occurring in the real process. The model considers an induction heating coil, consolidation roller and cooling air-jet nozzle which traverse a total distance of 300 mm and create the conditions necessary for the fusion bonding of two composite (CF-PPS) laminate materials. The structural mechanics includes roller contact and a moving radial pressure which has also been included to account for the force generated by a cooling air-jet. The models have been used to investigate welding temperature processing windows and potential optimization strategies that can help this method reach the process speeds necessary for it to be implemented in mass production scenarios. Further work continues to see what can be done in the area of process control and the implementation of a suitable control system for the process.

ACKNOWLEDGEMENTS

The authors would like to thank Mr. Arthur Shapiro for the keyword function code which defines the cooling air-jet moving convection boundary condition and also Mr. Isheng Yeh for the implementation of the sensor keyword options allowing the detection of max temperature in a part used by the PID controller function.

REFERENCES

[1] D. Grewell, A. Benatar and J. Park. *Plastics and Composites Welding Handbook*. Hanser, München, 2003.

[2] V. Rudnev, D. Loveless, R. Cook and M. Black. *Handbook of Induction Heating*. Marcel Dekker, New York, USA, 2003.

[3] A.C. Loos, M.-C Li. *Processing of composites: Consolidation during thermoplastic composite processing*. Hanser, Munich, 2000.

[4] W.I. Lee, G.S. Springer. *A Model of the Manufacturing Process of Thermoplastic Matrix Composites*. Journal of Composite Materials, 21(11):1017-1055, 1987.

[5] F. Yang, R. Pitchumani. *Fractal Description of Interlaminar Contact Development during Thermoplastic Composites Processing*. Journal of Reinforced Plastics and Composites, 20(7):536-546, 2001.

[6] F. Yang, R. Pitchumani. *Interlaminar contact development during thermoplastic fusion bonding*. Polymer Engineering & Science, 42(2):424-438, 2002.

[7] F. Yang, R. Pitchumani. *Healing of Thermoplastic Polymers at an Interface under Nonisothermal Conditions*. Macromolecules, 35(8):3213-3224, 2002.

[8] R. Rudolf, P. Mitschang, M. Neitzel. *Induction heating of continuous carbon-fibre-reinforced thermoplastics*. Composites Part A 2000; 31: 1191–1202.

[9] L. Moser, P. Mitschang. *Experimental Analysis and Modeling of Susceptorless Induction Welding of High Performance Thermoplastic Polymer Composites*, PhD thesis, Institute für Verbundwerkstoffe GmbH, Kaiserslautern, Germany, 2012.

[10] M. Duhovic, I. Caldichoury, P. L'Eplattenier, P. Mitschang, M. Maier. *Advances in Simulating the Joining of Composite Materials by Electromagnetic Induction*. In: Proceedings of the 9th European LS-DYNA® Users Conference, Manchester, 2013.

[11] M. Duhovic, L. Moser, P. Mitschang, M. Maier, I. Caldichoury, P. L'Eplattenier. *Simulating the Joining of Composite Materials by Electromagnetic Induction*. In: Proceedings of the 12th International LS-DYNA® Users Conference, Electromagnetic (2), Detroit, 2012.